Large amplitude spatial and temporal gradients in atmospheric boundary layer CO_2 mole fractions detected with a tower-based network in the U.S. upper Midwest

Natasha L. Miles,[1] Scott J. Richardson,[1] Kenneth J. Davis,[1] Thomas Lauvaux,[1] Arlyn E. Andrews,[2] Tristram O. West,[3] Varaprasad Bandaru,[3] and Eric R. Crosson[4]

Received 1 June 2011; revised 12 December 2011; accepted 17 December 2011; published 21 February 2012.

[1] This study presents observations of atmospheric boundary layer CO_2 mole fraction from a nine-tower regional network deployed during the North American Carbon Program's Mid-Continent Intensive (MCI) during 2007–2009. The MCI region is largely agricultural, with well-documented carbon exchange available via agricultural inventories. By combining vegetation maps and tower footprints, we show the fractional influence of corn, soy, grass, and forest biomes varies widely across the MCI. Differences in the magnitude of CO_2 flux from each of these biomes lead to large spatial gradients in the monthly averaged CO_2 mole fraction observed in the MCI. In other words, the monthly averaged gradients are tied to regional patterns in net ecosystem exchange (NEE). The daily scale gradients are more weakly connected to regional NEE, instead being governed by local weather and large-scale weather patterns. With this network of tower-based mole fraction measurements, we detect climate-driven interannual changes in crop growth that are confirmed by satellite and inventory methods. These observations show that regional-scale CO_2 mole fraction networks yield large, coherent signals governed largely by regional sources and sinks of CO_2.

Citation: Miles, N. L., S. J. Richardson, K. J. Davis, T. Lauvaux, A. E. Andrews, T. O. West, V. Bandaru, and E. R. Crosson (2012), Large amplitude spatial and temporal gradients in atmospheric boundary layer CO_2 mole fractions detected with a tower-based network in the U.S. upper Midwest, *J. Geophys. Res.*, *117*, G01019, doi:10.1029/2011JG001781.

1. Introduction

[2] Interest in quantifying carbon dioxide (CO_2) sources and sinks, both biogenic and anthropogenic, is growing with the increasing interest in monitoring and verifying CO_2 emissions [*Committee on Methods for Estimating Greenhouse Gas Emissions*, 2010]. The continuous tower-based CO_2 mole fraction measurement density is increasing in the United States and Europe, with the goal of using the data in inversion models to diagnose CO_2 fluxes. In North America, 6–8 towers within an area of 10^7 km^2 were available to past continental-scale studies [*Peylin et al.*, 2005; *Peters et al.*, 2007; *Schuh et al.*, 2010]. Other studies focused on regional scales, using CO_2 mole fractions measured at one tower in addition to aircraft [*Matross et al.*, 2006] and meteorological [*Tolk et al.*, 2009] data. *Lauvaux et al.* [2009], using data observed during the CarboEurope Regional Experiment [*Dolman et al.*, 2006], determined regional-scale fluxes using two towers within a 10^5 km^2 domain, representing an order of magnitude improvement in tower density. Still, the scarcity and limited time frame of tower-based measurements have hindered the determination of regional-scale fluxes [*Matross et al.*, 2006]. Uncertainties in the flux estimates remain large, but can be reduced by including additional towers [*Butler et al.*, 2010].

[3] The Mid-Continent Intensive (MCI) is the first targeted experimental campaign of the North American Carbon Program (NACP) [*Wofsy and Harriss*, 2002; *Denning*, 2005]. The primary objective of the MCI [*Ogle et al.*, 2006] is to compare regional-scale CO_2 fluxes derived from inventory data and biogeochemical models [*King et al.*, 2007; *Xiao et al.*, 2008; *West et al.*, 2008; *Gurney et al.*, 2009; *Ogle et al.*, 2010] to fluxes inferred from tower-based CO_2 measurements via inversion models [*Tans et al.*, 1990; *Peters et al.*, 2007; *Lauvaux et al.*, 2009; *Schuh et al.*, 2010]. The MCI campaign incorporates tower CO_2 mole fraction measurements at nine sites, USDA National Agricultural Statistics inventory data, ongoing eddy-covariance flux measurements from AmeriFlux towers in the region, other inventory data such as the Vulcan fossil fuel emissions product [*Gurney et al.*, 2009], USDA National Resources Inventory, USDA Forest Inventory and Analysis data, and airborne trace gas measurements [*Martins et al.*, 2009; *Crevoisier et al.*, 2010].

[1]Department of Meteorology, Pennsylvania State University, University Park, Pennsylvania, USA.
[2]Earth System Research Laboratory, Global Monitoring Division, National Oceanic and Atmospheric Administration, Boulder, Colorado, USA.
[3]Pacific Northwest National Laboratory, Joint Global Change Research Institute, University of Maryland, College Park, Maryland, USA.
[4]Picarro, Inc., Sunnyvale, California, USA.

0148-0227/12/2011JG001781

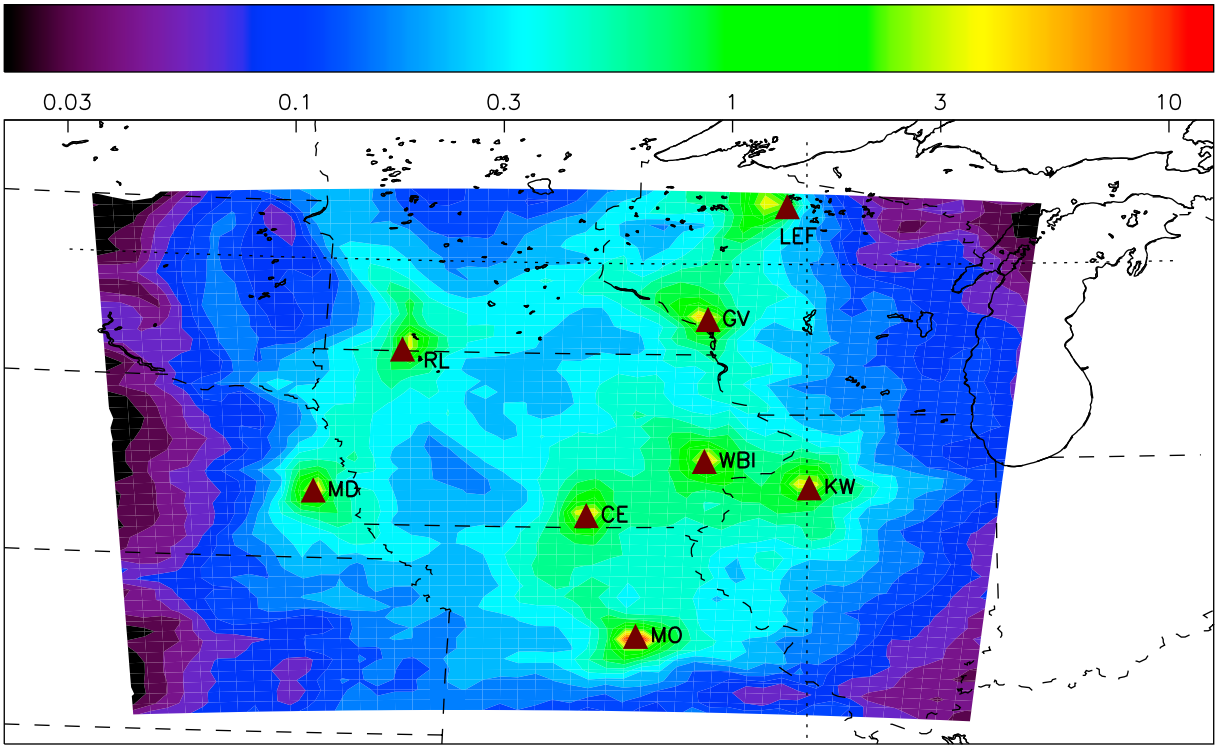

Figure 1. Footprint of the CO_2 mixing ratio tower network plotted on a natural logarithmic scale. The footprints (ppm/g CO_2 m^{-2} h^{-1}) are normalized such that the total is 100% times the number of towers; the color bar indicates the approximate percentage of the contribution (within the MCI domain) arising from each particular 20 km × 20 km pixel. The time frame is July–August 2007.

[4] Modeling results for the MCI region show the importance of vegetation type. Simulation of corn and soybean explicitly using crop-specific physiology and phenology results in improved modeled NEE [*Lokupitiya et al.*, 2009] and forward modeled CO_2 mole fractions [*Corbin et al.*, 2010]. While *Lauvaux et al.* [2011] present the regional CO_2 fluxes for June–December 2007 and explore model uncertainties resulting from inverse system assumptions, in this paper we focus on the CO_2 mole fraction measurements.

[5] Understanding of the characteristics (amplitudes, temporal persistence, and attribution to vegetation, weather, and climate) of atmospheric CO_2 is critical to the design of observational networks [*Committee on Methods for Estimating Greenhouse Gas Emissions*, 2010; *Nisbet and Weiss*, 2010]. Documenting the characteristics and causes of transient, weather-related regional mole fraction gradients has not, however, been possible to date because of very limited spatial sampling. Seasonal-scale characteristics have been previously reported at single sites [*Davis et al.*, 2003; *Haszpra et al.*, 2008] but not for a regional network. Previous studies of daily scale gradients have largely been limited to temporal analyses at single sites [*Hurwitz et al.*, 2004], modeling [*Wang et al.*, 2007] and aircraft studies [*Chan et al.*, 2004; *Gerbig et al.*, 2003]. While there are numerous satellite remote sensing design studies [*Houweling et al.*, 2010], real data to inform these studies are scarce [*Lin et al.*, 2004].

[6] The purposes of this paper are (1) to document the seasonal cycle of CO_2 mole fraction at several sites in a largely agricultural region; (2) to document the spatial CO_2 mole fraction gradients in the region on seasonal, daily, and interannual time scales; (3) to ascertain the degree to which regional-scale CO_2 mole fraction networks can yield coherent signals governed largely by regional sources and sinks of CO_2; and (4) to determine if signals in the tower-based CO_2 mole fraction data are correlated with both ground-based inventory data and estimates from satellite remote sensing.

2. Methods

2.1. Mid-Continent Intensive Region

[7] The U.S. upper Midwest (Figure 1) was the region selected for the Mid-Continent Intensive (MCI) because of its uncomplicated terrain and because the dominant crop ecosystems are extensively documented. The region is primarily agricultural, with cropland and grassland being the dominant vegetation types, but has forest cover in the southern and especially northern portions of the region (U.S. Geological Survey Land Cover Institute, 2010; see http://landcover.usgs.gov). Corn and soybeans are the dominant crops; in Iowa, the area planted with these crops is 52% and 41% of the total agricultural area, respectively [*U.S. Department of Agriculture National Agricultural Statistics Service* (*USDA-NASS*), 2010].

2.2. Tower CO_2 Measurements

[8] A total of nine communication tower-based CO_2 sensors were located within a 500 × 800 km^2 area within the MCI study region from May 2007 through November 2009

Table 1. Site Latitudes, Longitudes, Measurement Dates, and Sampling Level Used

	Centerville	Galesville	Kewanee	Mead	Missouri Ozarks	Round Lake	Rosemount	West Branch	Park Falls
Latitude (deg N)	40.7919	44.0910	41.2762	41.1386	38.7441	43.5263	44.6886	41.725	45.9459
Longitude (deg W)	92.8775	91.3382	89.9724	96.4559	92.2000	95.4137	93.0728	91.353	90.2723
Measurement dates	Apr 2007 to Nov 2009	Jun 2007 to Nov 2009	Apr 2007 to Nov 2009	Apr 2007 to Nov 2009	Sep 2006 to current	May 2007 to Nov 2009	Nov 2007 to current	Jul 2007 to current	1995 to current
Sampling level used (m AGL)	110	122	140	122	30	110	100	99	122

(see Table 1 and Figure 1). The mean distance of each tower to the closest neighboring tower is 188 km (Table 2). The National Oceanic and Atmospheric Administration (NOAA)'s Earth System Research Laboratory (ESRL) maintains measurements of CO_2 mole fractions at two long-term tall towers in the study region (LEF, Park Falls, Wisconsin, and WBI, West Branch, Iowa). These sites are part of the NACP's continental backbone observing network and serve as foci for the MCI experiment. LEF (Park Falls, Wisconsin) and WBI (West Branch, Iowa) are instrumented with NOAA-ESRL tall tower nondispersive infrared (NDIR) systems [*Bakwin et al.*, 1995; *Zhao et al.*, 1997]. With the goal of oversampling the MCI region, The Pennsylvania State University deployed instruments at five towers: Centerville (Iowa), Galesville (Wisconsin), Kewanee (Illinois), Mead (Nebraska), and Round Lake (Minnesota). These sites were instrumented with wavelength-scanned cavity ring-down spectroscopy (WS-CRDS) systems (Picarro, Inc., Santa Clara, California, model CADS) [*Crosson*, 2008]. *Chen et al.* [2010] document the accuracy and precision of a

Table 2. Distances Between Site Pairs, Magnitudes of the Median Intersite Differences and Gradients in Daily Daytime CO_2 Mole Fraction[a]

	Centerville	Galesville	Kewanee	Mead	Missouri Ozarks	Round Lake	Rosemount	West Branch	Park Falls
				Centerville					
Distance (km)		388	250	303	235	369	437	164	611
Median difference (ppm)		0.58	5.13	0.88	1.50	6.04	4.08	5.12	0.15
Median gradient (ppm/100 km)		0.2	2.1	0.3	0.6	1.6	0.9	3.1	0.0
				Galesville					
Distance (km)			332	532	600	333	156	263	223
Median difference (ppm)			4.45	0.51	2.84	5.43	0.60	3.96	1.43
Median gradient (ppm/100 km)			1.4	0.1	0.5	1.6	0.4	1.5	0.6
				Kewanee					
Distance (km)				543	340	512	459	125	520
Median difference (ppm)				5.37	7.42	0.48	3.04	0.97	6.43
Median gradient (ppm/100 km)				1.0	2.2	0.1	0.7	0.8	1.2
					Mead				
Distance (km)					450	279	483	430	730
Median difference (ppm)					0.17	5.14	1.36	4.73	0.11
Median gradient (ppm/100 km)					0.0	1.8	0.3	1.1	0.0
						Missouri Ozarks			
Distance (km)						597	669	340	817
Median difference (ppm)						9.02	5.89	8.44	4.13
Median gradient (ppm/100 km)						1.5	0.9	2.5	0.5
							Round Lake		
Distance (km)							228	388	487
Median difference (ppm)							4.72	1.22	6.47
Median gradient (ppm/100 km)							2.1	0.3	1.3
								Rosemount	
Distance (km)								361	260
Median difference (ppm)								1.84	0.67
Median gradient (ppm/100 km)								0.5	0.3
									West Branch
Distance (km)									477
Median difference (ppm)									6.02
Median gradient (ppm/100 km)									1.3

[a]Time period is 2007–2009 growing season (July and August). Sites are classified as either corn dominated (Kewanee, Round Lake, and West Branch), or non–corn dominated.

WS-CRDS (Picarro, Inc.) in laboratory testing and an aircraft deployment. *Richardson et al.* [2012] document the quality assessment of the instruments during the MCI; 8 months of testing against a NOAA-ESRL NDIR system in West Branch, Iowa, yielded median daytime-only differences of -0.13 ± 0.63 ppm. Two additional long-term sites measuring well-calibrated CO_2 mole fraction (University of Minnesota KCMP, Rosemount, Minnesota, and Pennsylvania State University (PSU)/Oak Ridge National Laboratory (ORNL, Missouri Ozarks, Missouri) are located within the region and used in this study. At the University of Minnesota Rosemount tower, CO_2 mole fraction is measured using a tunable diode laser [*Griffis et al.*, 2010]. The Missouri Ozarks CO_2 measurement site is colocated with an ongoing AmeriFlux site [*Gu et al.*, 2008] and employs a well-calibrated system based on a NDIR instrument (Licor, Inc., Lincoln, Nebraska, model LI-820). The system is dried using Nafion (Perma Pure, LLC, Toms River, New Jersey, model MD-070-96P-4) driers, calibrated every 4 h using four real-air standards (with hourly target and daily archive tests as well), temperature and pressure controlled, and automatically leak tested. Residuals from known tank values tested daily at the site are -0.11 ± 0.21 ppm [*Stephens et al.*, 2011].

[9] Although nighttime mole fractions provide useful information about respiration, in this study we focus on only the daytime (12:00–17:00 LST) average CO_2 mole fractions. Although these hours extend into the evening transition as defined by *Davis et al.* [2003], composited diurnal cycles of CO_2 in July are well mixed during these hours [*Bakwin et al.*, 1998, Figure 1]. During the daytime, the CO_2 mole fraction from the levels used in this study (100–140 m AGL for all sites except for Missouri Ozarks, which is 30 m AGL) is a reasonable approximation of the mixed layer value [*Bakwin et al.*, 1998; *Chan et al.*, 2004]. At West Branch during daytime in the peak growing seasons 2007–2009, the median difference between the 99 and 379 m AGL values is 1.0 ± 2.2 ppm and between the 31 and 99 m AGL values is 1.1 ± 1.5 ppm.

[10] To investigate seasonal-scale variability, we used a 31 day running mean to smooth the CO_2 mole fraction daily daytime average data. We required 60% of the days within each window to be good data. To avoid extending the smoothed product over areas with prolonged missing data, we also required that there be good data within 2 days of each smoothed point.

2.3. Tower Mole Fraction Footprints

[11] We simulated the tower mole fraction footprints using the nonhydrostatic mesoscale model WRF-Chem v3.1 [*Skamarock et al.*, 2008] at 10 km resolution. The WRF simulations used are described in more detail in the work of *Lauvaux et al.* [2011], but here we summarize the description of the main schemes, driver data, and resolution. The atmospheric boundary layer scheme used is the Mellor-Yamada-Nakanishi-Niino (MYNN) 2.5 scheme coupled to the Monin-Obukhov (Jancic Eta) scheme for the surface physics. The atmospheric vertical column is described by 60 levels, with 40 levels in the lower 2 km. We used the NOAH land surface model to describe the surface energy balance, and the NCEP Eta/NAM model output at 40 km resolution for the initial conditions and nudged over four pixels (40 km) to provide boundary conditions around our simulation domain. We simulated the influence functions with the Lagrangian Particle Dispersion Model [*Uliasz*, 1994]. We used the mean three-dimensional winds, potential temperature, and turbulent kinetic energy as input variables each 30 min to drive the particle motions from the receptor locations to the sources, as described in the work of *Lauvaux et al.* [2008]. We computed the footprints for each observation hour, at each tower location, by counting particles over a 20 km resolution grid. We then averaged the footprints corresponding to daytime hours only (06:00–18:00 LST) at a weekly time step, and summed over July–August 2007 to represent the area of influence at the surface during the growing season. The resulting summer time aggregated footprint represents the contribution of each surface pixel within the MCI domain to the summer drawdown observed in the daily daytime mole fractions. In addition, we quantified the influence of the boundaries (CO_2 mole fraction inflow) by counting particles at the boundaries. The boundary influence is a separate contribution, given by a global-scale model, in this case, CarbonTracker 2009 [*Peters et al.*, 2007]. We thus computed the fractional influence from outside the MCI domain, as well as the distribution of the influence within in it.

2.4. Vegetation Map

[12] The vegetation map we used in calculating the biome fractional influence is similar to that described in the work of *Schuh et al.* [2010]. We obtained biomes from the Terra MODIS 12 Landcover 1 km product and mapped them to SiB biome classes, with corrections for C4 grasses. We disaggregated corn, soy, and wheat biomes from the original grassland/agriculture biome using county-level estimates of land use from the USDA National Agriculture Statistics Service. The new grassland/agriculture (C3) category thus includes crops such as alfalfa hay and oats as well as the more predominant pastureland. Tallgrass (C4) prairie and wheat are not predominant in the MCI region, and are included in the "other" category. Forested biomes were combined. The final vegetation map includes the fractional coverage of the four most represented biomes in the MCI region with an additional category for all other biomes (forest, soy, grassland, corn, and other) at 1 km resolution. In section 3.1 this map is combined with 20 km resolution footprints to represent the fractional influence at the towers for each of the five categories.

2.5. NDVI Time Series Crop Phenology Curves

[13] The Normalized Difference Vegetative Index (NDVI) was estimated using 250 m spatial resolution, 8 day composite, collection-5 reflectance data (MOD09Q1) from NASA's Terra Moderate Resolution Imaging Spectroradiometer (MODIS) sensor. MODIS reflectance data is corrected for atmospheric gases and aerosols [*Vermote et al.*, 2002], and has high subpixel geolocation accuracy [*Wolfe et al.*, 2002]. MOD09Q1 reflectance data consists of observations that are selected on the basis of quality, view angle, and absence of clouds [*Vermote et al.*, 2011]. MOD09Q1 also includes binary quality control flags that provide information on pixel quality. We used the quality control information to select high-quality, cloud-free data from days

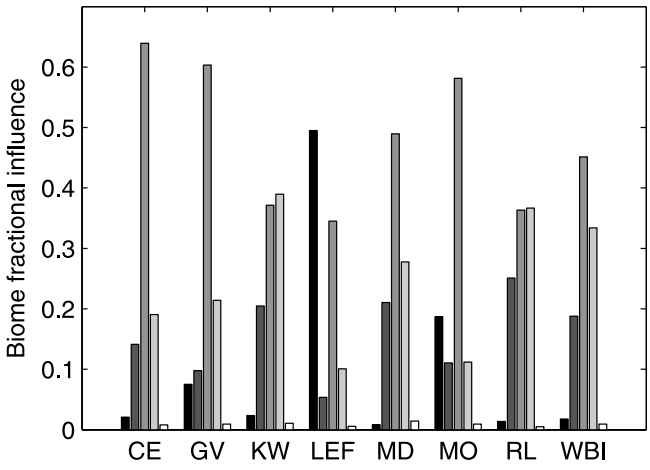

Figure 2. Biome fractional influence, averaged over July–August 2007, for the daytime only (not available for Rosemount). The biomes include, from left to right: forest, soy, grassland, corn, and other.

81–321 for years 2007–2009. The tiled reflectance data was mosaicked and then reprojected from Sinusoidal to Albers Equal-Area Conic Projection using the MODIS Reprojection Tool (MRT) [*Dwyer and Schmidt*, 2006]. The Cropland Data Layer (CDL), an annual crop-specific land cover data set based on satellite data [*Johnson and Mueller*, 2010], was used to retrieve reflectance data from MOD09Q1 for corn and soybean crops. NDVI was calculated for each composited day and for each crop, and then combined to generate time series crop phenology curves for years 2007–2009. Positive and negative changes in the slope of the phenology curves represent plant emergence and senescence, while plant maturity occurs at peak NDVI.

3. Results

3.1. Atmospheric- and Inventory-Based Detection of CO_2 Flux Spatial Variability

[14] Before examining the CO_2 mole fraction measured in the MCI, we first consider the spatial areas that contribute to the signal measured at each tower. Mole fraction footprints, when combined with the spatially varying flux, indicate the relative influence of a location at the surface to the mole fraction measured at a tower. July–August 2007 averaged, daytime-only footprints are shown in Figure 1 for the MCI towers. About 39% of the total signal (ΔCO_2/flux) originates with a 150 km radius of each tower. Conversely, 28% originates outside of the MCI domain. The signal per unit area decreases quickly with distance from the towers: pixels surrounding each of the towers each contribute 1–3% of the total signal, while pixels on the edge of the domain each contribute two orders of magnitude less per pixel to the total signal (Figure 1).

[15] We now couple the footprints with the vegetation map described in section 2.4 to determine the biome fractional influence (Figure 2), a measure of the fractional time that an air parcel arriving at each tower has spent influenced by each biome. The contribution of each biome varies considerably among the sites. Grassland, which includes alfalfa and oats as well as the more predominant pastureland, is the biome most influencing Centerville, Galesville, and Mead. Park Falls (LEF) and Missouri Ozarks are influenced primarily by forest and grassland biomes. Although corn influences each site, the contribution is largest at Kewanee, Round Lake, and West Branch. Soybeans, while common in the region, do not dominate the influence of any of the sites. Wheat and tallgrass prairie are not common in the MCI region.

[16] The variability in the predominant vegetation types of the region affects the regional patterns in CO_2 flux because of the variability of carbon uptake per unit area of each vegetation type. Shown in Figure 3 is the weekly averaged daytime (12:00–17:00 LST) net ecosystem exchange (NEE) measured at four corn (Rosemount-G19 in Minnesota; see *Griffis et al.* [2010] and Mead-rain, Mead-irrigated, and Mead-irrigated/rotated in Nebraska; see *Verma et al.* [2005]), two grassland (Brookings and Fermi prairie in Illinois; see *Matamala et al.* 2008]), two forest (LEF in Wisconsin; see *Davis et al.* [2003] and Missouri Ozarks in Missouri; see *Gu et al.* [2008]), and one soy (Fermi agriculture in Illinois; see *Matamala et al.* [2008]) eddy-covariance flux sites in the MCI region. The peak daytime NEE of corn during the growing season is significantly larger than that of each of the other vegetation types. The peak daytime NEE over the year for the corn sites occurs in mid-July, averaging -51 μmol m^{-2} s^{-1} for the four corn sites. The average of the Mead corn sites in 2001/2003 is -63 μmol m^{-2} s^{-1} [*Verma et al.*, 2005]. In 2002, two of the Mead sites were planted with soybean and their peak CO_2 uptake averages -37 μmol m^{-2} s^{-1} [*Verma et al.*, 2005]. In summary, using the peak daytime weekly averaged NEE for site-years shown in Figure 3 in addition to the results in the work of *Verma et al.* [2005], the corn/soy peak NEE ratio varies between 1.4 and 3.2, the corn/grassland peak NEE ratio varies between

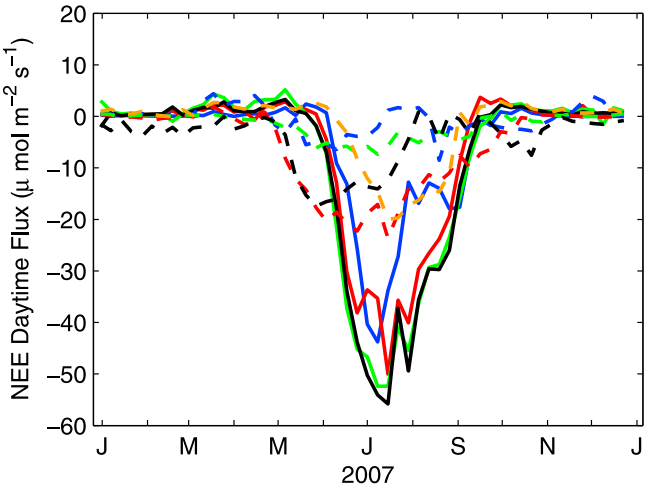

Figure 3. Weekly averaged daytime (12:00–17:00 LST) net ecosystem exchange measured at corn-dominated eddy flux sites Rosemount-G19 (blue solid line), Mead-rain (red solid line), Mead-irrigated (green solid line), and Mead-irrigated/rotated (black solid line); grassland-dominated sites Brookings (blue dotted line) and Fermi-prairie (red dotted line); forested sites LEF (green dotted line) and Missouri Ozarks (black dotted line); and soy site Fermi-agriculture (orange dotted line).

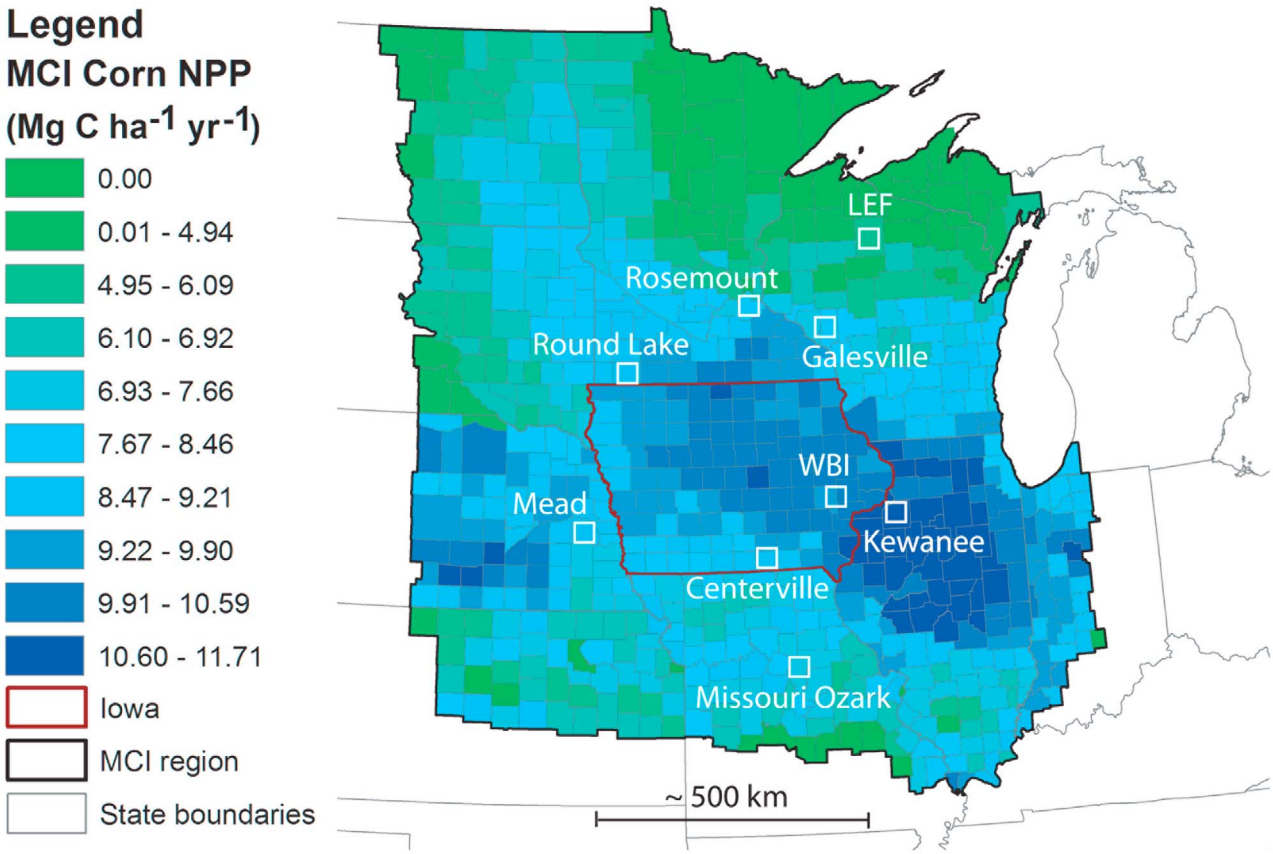

Figure 4. Inventory-based corn flux (corn NPP) in the MCI region for 2007, including corn grain and corn silage. Tower-based CO_2 mixing ratio measurement site locations in the MCI region are shown (open squares). Map resolution is the county geopolitical unit.

2.3 and 7.0, and the corn/forest peak NEE ratio varies between 3.0 and 9.0. The large difference in NEE between corn and noncorn sites when the plants are growing contributes to the important role that corn plays in the carbon budget of this largely agricultural region.

[17] We now consider the net primary production (NPP) for corn in the MCI region, derived from USDA National Agricultural Statistics Service inventory data based on methods described by *West et al.* [2010]. Areas of highest corn flux per unit area are in Nebraska, southern Minnesota, Iowa, and northern and central Illinois (Figure 4). The corn NPP within the MCI region varies from about 5 to 10 Mg C ha^{-1} yr^{-1}, nearly doubling carbon uptake when moving from southeast Iowa to northwest Iowa. We describe the three sites with corn fractional influence greater than 0.30 (Kewanee, Round Lake, and West Branch) as "corn dominated" and the remaining six as "non–corn dominated" to reflect the differences in corn fractional influence and corn NPP per unit area. The threshold of 0.30 was chosen to minimize the sum of the standard deviations of the corn fractional influence within the two groups, requiring each group to have at least three members.

[18] From the above results, we have inferred regional patterns in ecosystem NEE. We now determine whether these patterns are apparent in the CO_2 mole fractions measured at the towers, or if, instead, atmospheric mixing equilibrates the gradients. In the smoothed time series of CO_2 mole fraction (Figure 5), the corn-dominated sites in fact exhibit extremely low growing season minima, in the range of 358–364 ppm. These low values are near those last observed in the globally averaged marine surface annual CO_2 mole fractions 10–13 years prior to the beginning of this study (see http://www.esrl.noaa.gov/gmd/cgg/trends). The growing season minima are correlated with the relative influence of corn, with the corn-dominated minima average 6–8 ppm lower than the non-corn-dominated average (Table 3). Similarly, the seasonal drawdown (the difference between dormant season maxima and growing season minima for each year) also varies within the MCI region. The seasonal drawdown averages 35 ppm for corn-dominated sites (Table 3), which is significantly larger than that measured at non–corn belt sites (27 ppm), and is 5 times larger than the tropospheric "background" as represented by Mauna Loa (7 ppm). Aircraft-measured free tropospheric CO_2 mole fractions at WBI also exhibit a 7 ppm drawdown (see http://www.esrl.noaa.gov/gmd/cgg/trends). The corn-dominated seasonal drawdown is larger than that previously observed at continental boundary layer sites, for example, 26 ppm at Hegyhátsál [*Haszpra et al.*, 2008] and 23 ppm at LEF [*Davis et al.*, 2003]. Although Centerville, Galesville, Mead, and Rosemount have a large influence from crops, the CO_2 seasonal pattern of those sites is more similar to the forested sites LEF and Missouri Ozarks (Figure 5).

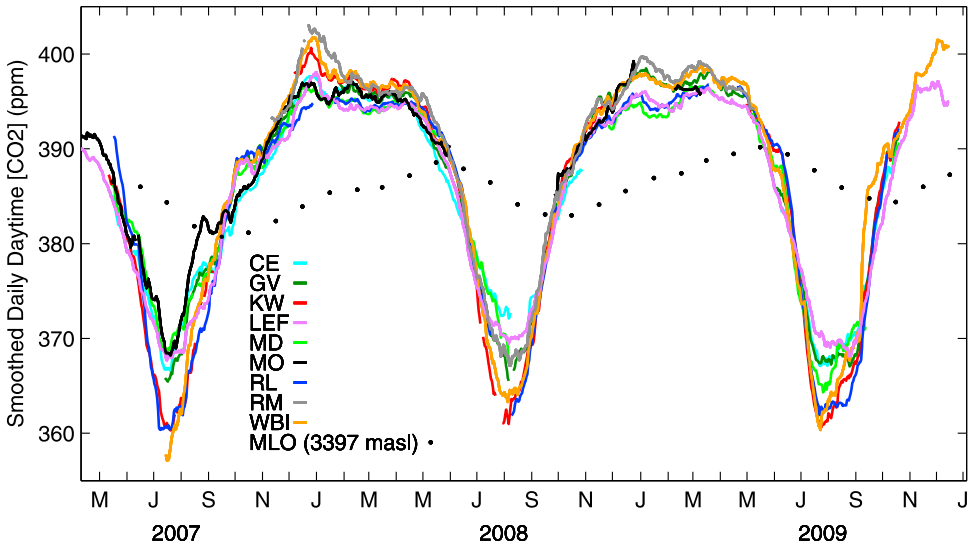

Figure 5. Smoothed CO_2 mole fraction for each site in the MCI region. Data for Mauna Loa (MLO), representing the tropospheric "background," are shown for reference (data courtesy of NOAA-ESRL; see http://www.esrl.noaa.gov/gmd/cgg/trends). Rosemount data are courtesy of T. Griffis (University of Minnesota).

[19] We now consider the magnitude of the seasonal drawdown expected because of the differing NEE from each biome. As a first-order estimate, the magnitude expected is proportional to the sum of the fractional influence of each biome multiplied by the average biome flux. The average corn, soy, grass, and forest fractional influence for corn-dominated sites is 0.36, 0.21, 0.39, and 0.02, respectively, whereas for non-corn-dominated sites the fractional influence is 0.18, 0.12, 0.53, and 0.16 (Figure 2). Using a range of values for each corn/noncorn biome NEE ratio (Figure 3), the expected ratio between the average seasonal drawdown of the corn-dominated versus the non-corn-dominated sites is 1.29–1.56. The actual ratio is 1.26 (Table 3). Since our estimate excludes the effects of atmospheric mixing, it is not surprising that the actual ratio is near the lower extreme of the estimate. A more precise analysis is prohibited by lack of knowledge of the exact corn/noncorn flux ratios.

[20] As is apparent in Figure 5, on a seasonal timescale, gradients observed across the region are strongly dependent on local vegetation type. We consider spatial differences and gradients of two different groups of site pairs: similar vegetation site pairs (either both corn dominated or both non–corn dominated), and cross-vegetation site pairs (one corn-dominated site paired with one non-corn-dominated site). Distributions of the differences and gradients for two similar vegetation site pairs and two cross-vegetation site pairs are shown in Figure 6. The magnitude of the median intersite difference for pairs including only similar vegetation types

Table 3. Dormant Season Maxima, Growing Season Minima, and Seasonal Drawdown of the Smoothed CO_2 Mole Fraction for Each Site Compared to Reference Values of 395 and 360 ppm[a]

		2007			2008			2009		
Site	Rank in Terms of Corn Biome Influence	Dormant Season Maxima	Growing Season Minima (ppm)	Seasonal Drawdown[b]	Dormant Season Maxima	Growing Season Minima (ppm)	Seasonal Drawdown[b]	Dormant Season Maxima	Growing Season Minima (ppm)	Seasonal Drawdown[b]
Park Falls	9	–	8	25[c]	−1	10	24	1	9	27
Missouri Ozarks	8	–	8	26[c]	0	–	–	1	–	–
Centerville	7	–	7	27[c]	0	13	22	–	7	29[c]
Galesville	6	–	6	29[c]	1	7	29	2	7	30
Rosemount	5	–	–	–	1	8	28	–	–	–
Mead	4	–	9	24[c]	−1	7	27	1	4	32
West Branch	3	–	−2	38[c]	2	4	33	3	0	38
Round Lake	2	–	1	32[c]	−1	3	31	1	3	33
Kewanee	1	–	1	34[c]	1	2	34	–	1	36[c]
Reference value		–	360	–	395	360	–	395	360	–

[a]For example, the actual dormant season maxima for Park Falls is 395 + (−1) = 394 ppm. The sites are ordered according to corn biome influence (Figure 2). Although the values are higher in January for 2007, we consistently use April values for the dormant season maxima for comparability.
[b]Seasonal drawdown is calculated by subtracting the growing season minima from each year's dormant season maxima.
[c]In site-years with missing dormant season maxima; the value was estimated by adding (subtracting) the difference between the 2008 and 2009 site-averaged dormant season maximum to (from) the site's 2008 dormant season maximum.

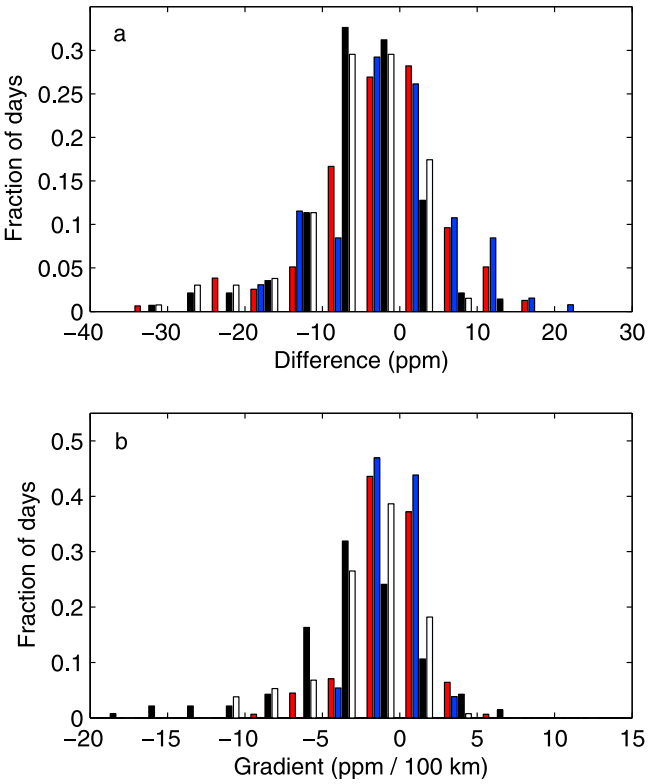

Figure 6. (a) The 2007–2009 averaged peak growing season (July–August) distribution of daily daytime average CO_2 mole fraction differences between Galesville and Centerville (red), Round Lake and Kewanee (blue), West Branch and Centerville (black), and Kewanee and Centerville (white). The bin size is 5 ppm. (b) As in Figure 6a but for gradients rather than differences. The bin size is 2.5 ppm/100 km. For both Figures 6a and 6b, colored bars represent distributions of similar vegetation site pairs, and black and white bars represent distributions of cross-vegetation site pairs.

is 0.9 ppm (see Figure 7a and Table 2) during the peak growing season (July–August), whereas the median of the intersite differences for cross-vegetation pairs is 5.2 ppm, with clear separation between the two groups. The pattern is similar for the gradients (see Figure 7b and Table 2) with the median magnitude of similar vegetation site pairs being 0.3 ppm/100 km, and that of cross-vegetation pairs being 1.5 ppm/100 km. West Branch (corn dominated) and Centerville (non–corn dominated), sites separated by only 164 km, exhibited the largest median intersite peak growing season gradient, 3.1 ppm/100 km, with a median intersite difference magnitude of 5.1 ppm (Table 2).

[21] Although the categorization of corn-dominated and non-corn-dominated groups simplifies the discussion, the relationship holds for the individual sites as well. The biome fractional influence for corn, or the average amount of time air parcels eventually arriving at each tower spent above land planted with corn, is shown as a function of the seasonal drawdown for each site in Figure 8. Sites most influenced by corn have larger seasonal drawdown, with a coefficient of determination (r^2) of 0.59.

[22] Another explanation for the observed differences in seasonal drawdown could be meteorological differences if corn were preferentially planted in areas with larger than average temperatures (enhancing plant growth and thus CO_2 uptake) or lower winds (thus lower mixing). However, analysis of July–August 2007 NCEP Reanalysis Products air temperature and wind speed (see http://www.esrl.noaa.gov/psd/data/reanalysis/) revealed no correlation of average temperature at each site with its seasonal drawdown (r^2 = 0.01) and only a slight correlation of the average wind speed (r^2 = 0.1).

3.2. Daily Scale Variability of CO_2 Fluxes

[23] In the previous discussion, we focused on the seasonal-scale patterns of CO_2 mole fraction in the MCI region. We now consider the large day-to-day weather-related variability (shown for WBI in Figure 9a). As an example of a corn-dominated and a non-corn-dominated site, we examine the histograms of CO_2 mole fraction for WBI and LEF for July–August 2007 (Figure 9b). While there is considerable overlap between the histograms, the median CO_2 mole fraction for WBI is 365.1 ppm, compared to 371.1 ppm for LEF. The standard deviation of the distribution is larger at WBI (11.7 ppm) compared to LEF (6.3 ppm), and there are several days during the growing seasons of 2007–2009 in which the daytime average CO_2 mole fraction measured at WBI is in the range 340–350 ppm.

[24] Both local weather and the overall weather patterns affect the daily CO_2 mole fraction measured at a tower. As local weather conditions change from one day to the next,

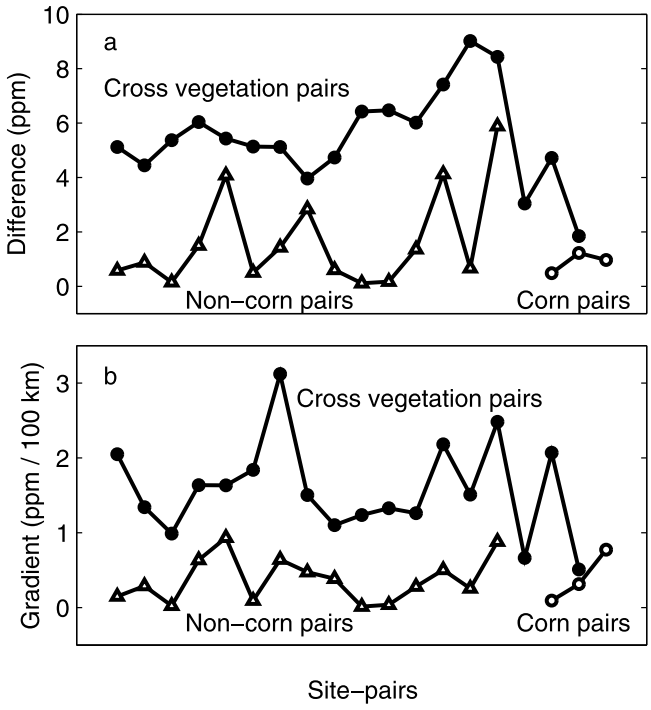

Figure 7. CO_2 mole fraction spatial differences and gradients. (a) Magnitude of the median intersite difference CO_2 mole fraction during the peak growing season (July–August 2007 to 2009) for pairs including only non-corn-dominated sites (triangles), pairs including only corn-dominated sites (open circles), and cross-vegetation pairs (solid circles). (b) Corresponding magnitude of the median intersite gradients.

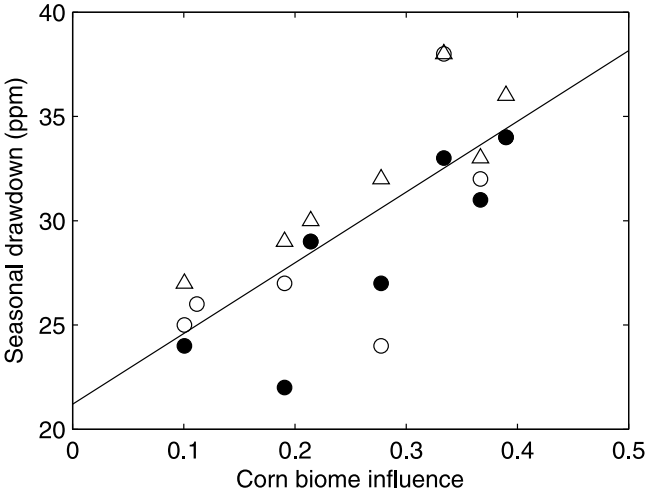

Figure 8. Fractional biome influence attributable to corn (as in Figure 2) as a function of seasonal drawdown (as in Table 3) in 2007 (open circles), 2008 (solid circles), and 2009 (triangles).

the fluxes are scaled accordingly, leading to daily changes in the CO_2 mole fractions. For example, *Chan et al.* [2004] showed that cloud cover in frontal regions reduces photosynthetic uptake, resulting in CO_2 mole fraction gradients across frontal regions. The CO_2 mole fractions of the air masses entering the region are dependent on their source region. A large-scale N–S gradient in near-surface CO_2 mole fractions exists between the largely agricultural MCI region and the relatively unproductive south-central United States (Texas/Louisiana/Oklahoma/Arkansas); the regional pattern of CO_2 mole fraction is thus dependent on large-scale wind direction [*Corbin et al.*, 2010].

[25] During the peak growing season (July–August), 5% of the day-to-day changes at individual sites are greater than 20 ppm and a few are greater than 30 ppm (Figure 10). While the day-to-day changes are large, they depend only weakly on local vegetation type: the mean magnitude is 7.3 ppm for corn-dominated sites, compared to 6.2 ppm for non-corn-dominated sites. Temporal changes and spatial gradients are inherently linked; the range of intersite gradients on a daily timescale is similarly only weakly dependent on local vegetation type. For similar vegetation site pairs, 9% of the gradients are larger than 5.5 ppm/100 km, and for cross-vegetation sites pairs 10% are. The contribution of the local flux to the CO_2 mole fraction spatial variability is thus dependent on timescale. While the daily scale CO_2 mole fraction depends most strongly on regional-scale weather conditions and air mass origin, when these daily values are averaged to a seasonal scale, we see the strong effects of the local flux as we showed in section 3.1.

3.3. Interannual Variability in CO_2 Fluxes

[26] The majority of sites exhibited relatively little change in their growing season minima from year to year. Some sites, however, showed interannual variability related to climate variability (Table 3). Flooding occurred in the midwestern United States during the first half of June 2008 (see http://www.ncdc.noaa.gov), although it was not uniform over the region. While Missouri Ozarks, Centerville, and West Branch recorded cumulative precipitation exceeding 30% above normal over the months of March–September, Round Lake, Rosemount, and Park Falls (LEF) experienced lower than normal precipitation during that time period. Two of the three sites experiencing the most flooding (Centerville and West Branch) exhibited decreased seasonal CO_2 drawdown (by 4–6 ppm) in 2008 as compared to 2007 and 2009. The vegetation of the flood-affected site that did not, Missouri Ozarks, includes a higher percentage of forest, which perhaps mitigated the flooding effects.

[27] Agriculture within the region was considerably affected by the 2008 flooding. Considering corn and soybeans together, the total harvested volume (grain production) of these crops decreased by 7% for the state of Iowa, compared to 2007 and 2009 [*USDA-NASS*, 2010]. The total estimated NPP of corn, using the method documented in the work of *West et al.* [2010], was 221.57, 207.33, and

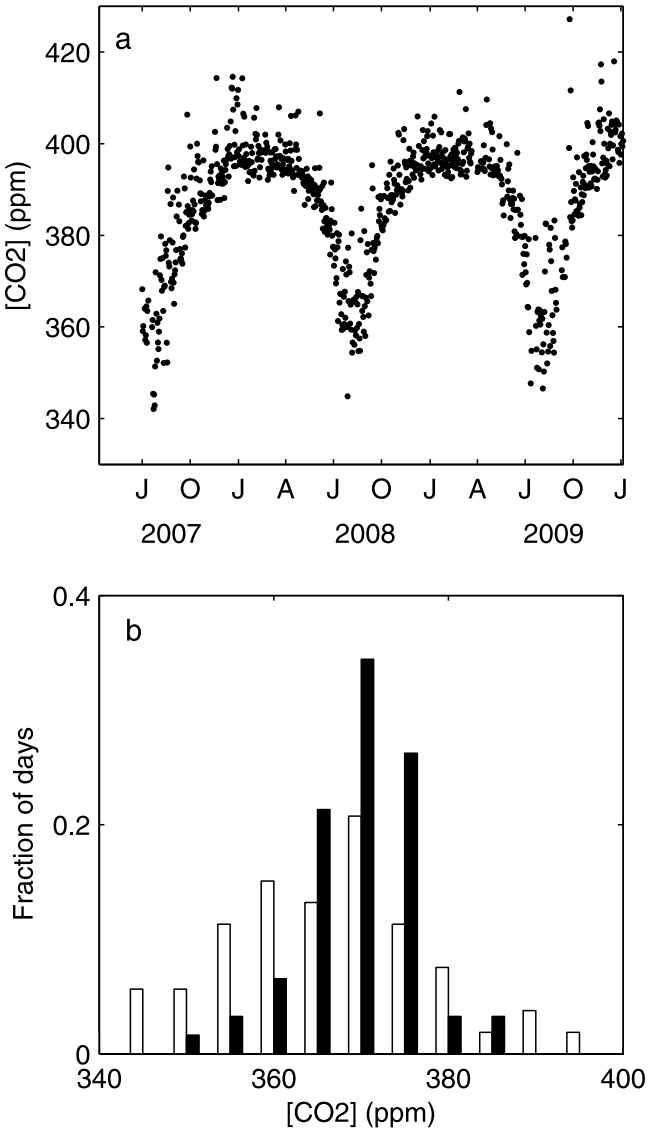

Figure 9. (a) Daily daytime CO_2 mole fraction for WBI. (b) Histogram of CO_2 mole fraction, for July–August 2007 only for WBI (white bars) and LEF (black bars). The bin size is 5 ppm.

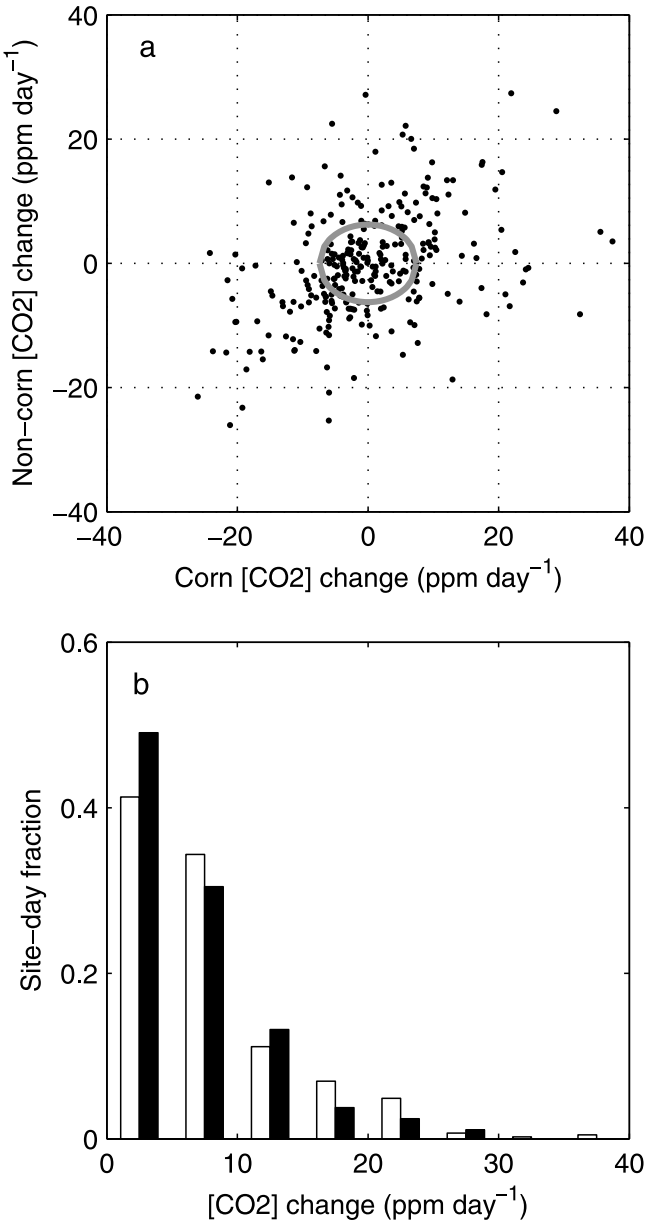

Figure 10. (a) The 2007–2009 peak growing season day-to-day change in daily daytime average CO_2 mole fraction observed at corn-dominated sites (WBI, KW, and RL) versus three of the non-corn-dominated sites (LEF, MO, and CE). Each point represents one day-to-day change for a cross-vegetation pair. The axes of the ellipse indicate the mean magnitude of the day-to-day change for the corn-dominated sites (7.3 ppm) and non-corn-dominated sites (6.2 ppm). (b) Histogram of the magnitude of the day-to-day changes in Figure 10a for corn-dominated sites (white bars) and non-corn-dominated sites (black bars).

222.52 Tg C in 2007, 2008, and 2009, respectively. Agricultural areas surrounding the Centerville site were most affected by the flooding of 2008, with corn harvested volume down by 18% compared to the 2007–2009 average, and soybean harvested volume down by 10% [*USDA-NASS*, 2010]. Other sites were affected by varying degrees. The total regional flux, of course includes contributions from natural ecosystems as well; they may be less affected by flooding.

[28] In addition to detecting effects of the 2008 flooding, we also see more subtle climate-based interannual variability, particularly in the timing of the crop growth. The onset of the growing season, as evidenced by the onset of the seasonal drawdown in CO_2, was 2–3 weeks early in 2007, compared to 2008 and 2009 (Figure 11a). Similarly, interannual differences are observed in the normalized difference vegetation index (NDVI) time series curves for corn and soybean fields in the State of Iowa. The emergence, maturity, and senescence of both corn and soy were late by 1–2 weeks in 2008 compared to 2007 (Figures 11b and 11c). Except for mid-June to mid-July, the 2009 corn NDVI followed that of 2008; soy NDVI for 2009 was similar to that of 2007 through August and then more similar to 2008. The coefficient of determination (r^2) between corn NDVI and smoothed atmospheric CO_2 mole fraction at Kewanee in 2007, 2008, and 2009 was 0.66, 0.85, and 0.75, respectively.

[29] Agricultural inventory statistics, based on farmer surveys [*USDA-NASS*, 2010], also indicate considerable interannual variability: corn in Iowa reached maturity about the same time in 2008 and 2009, but 3–4 weeks earlier in 2007. The spring of 2007 was particularly warm for the state

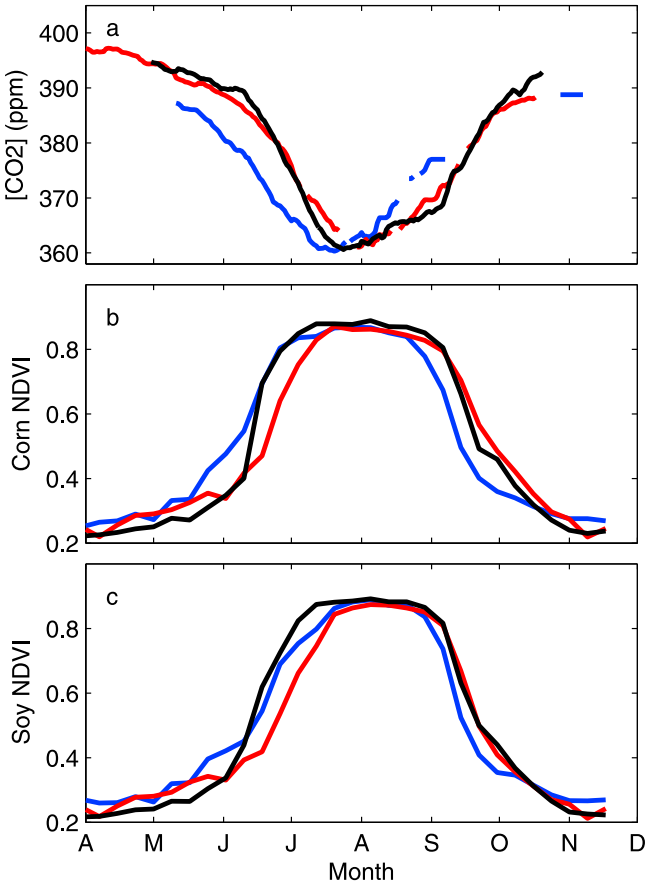

Figure 11. (a) Smoothed daily daytime average CO_2 mole fraction at Kewanee for 2007 (blue), 2008 (red), and 2009 (black). (b) Normalized difference vegetation index (NDVI) for corn averaged for the state of Iowa. (c) Same as Figure 11b but for soybeans.

of Iowa (above the 90th percentile for the period 1895–2009), whereas the springs of 2008 and 2009 were slightly below and near normal in temperature, respectively (see http://www.ncdc.noaa.gov). The summer of 2007 was near normal, 2008 was slightly below normal, and 2009 was below the 10th percentile in temperature. The warm spring of 2007, the flooding of 2008, and the cool summer of 2009 appear to have contributed to an early growing season with high NPP in 2007, a late growing season with low NPP in 2008, and a late growing season with high NPP in 2009, relative to each other. Thus, with a tower-based network of mole fraction measurements, we detect climate-driven interannual changes in crop growth timing that are confirmed via satellite and inventory methods.

[30] The separation between corn-dominated and non-corn-dominated sites in CO_2 mole fraction minima (Figure 5), while apparent in all three years, is most pronounced in 2007. This phenomenon, while possibly related to climate-induced variability, may also be related to crop management induced changes in the carbon flux. The acreage of corn planted in Iowa in 2007 increased in response to demand for ethanol production; the ratio of the area of corn planted to that of soy in 2007 was 1.61 compared to 1.33 and 1.46 in 2008 and 2009, respectively [*USDA-NASS*, 2010]. Additionally, *Griffis et al.* [2010] found a 10% increase in the contribution of corn to regional flux in the Rosemount area in 2007 compared to 2008. The increased separation between the CO_2 mole fraction minima could be explained if the footprints of the corn-dominated sites specifically included increased corn influence relative to the non-corn-dominated sites in 2007 compared to 2008 and 2009.

4. Implications for Atmospheric Verification of CO_2 Fluxes

[31] These observations show that, instead of being dominated by white noise, regional-scale CO_2 mole fraction networks obtain large, coherent signals. These signals are linked to both local vegetation and weather, and can be used in designing future observational networks. To put in perspective the magnitude of the spatial gradients observed in the MCI, we compare to ocean-continent values and to interhemispheric values, the mean annual spatial gradients that have been the traditional focus of atmospheric inversion studies. The ocean-continent gradient during the continental peak growing season [*GLOBALVIEW-CO2*, 2011] based on LEF is about 0.4 ppm/100 km. The annual interhemispheric mean difference for 2007–2009 is about 3.6 ppm [*GLOBALVIEW-CO2*, 2011]. The corresponding gradient is 0.036 ppm/100 km. The median gradient measured in the MCI region between cross-vegetation site pairs (1.5 ppm/100 km) is thus a factor of 4 times as large as the ocean-continent gradient and a factor of 40 times as large as the interhemispheric gradient. The atmosphere does not "mix out" these persistent and strong seasonal differences and gradients in the MCI region. It is therefore particularly important for regional, subseasonal inversion models to use accurate transport fields in areas like the MCI.

[32] The seasonal pattern in mole fractions across the region show persistent spatial structure that appears to be strongly dependent upon the dominance of corn, with implications for the footprint size, as well as for network design. The strong dependence of growing season median gradients on local vegetation type is consistent with the calculated footprint extents. Similarly, recent studies [*Lauvaux et al.*, 2008; *Gerbig et al.*, 2009] have documented the importance of the near field. Using synthetic data, *Lauvaux et al.* [2008] found significant error reduction in only about half of their 300 km $\times$ 300 km domain by including two towers. If the influence functions are integrated over the fluxes, the near-field effects can be stronger or weaker, depending on the surrounding vegetation. *Gerbig et al.* [2009], for August 2002 measurements at Harvard Forest, reported that the fluxes in the nearest 20–60 km contribute about half of the total, representing a larger near-field influence than shown in the current study. Centerville and West Branch, towers separated by only 164 km, differed in terms of seasonal-scale CO_2 patterns, with a median intersite peak growing season gradient of 3.1 ppm/100 km. These large gradients corroborate the importance of the near field. The implication of the two distinct groups (corn dominated and non–corn dominated) in the current study for network design is that tower locations should be distributed on the basis of prior ground-based fluxes, rather than homogenously distributed on the basis of statistical footprints.

[33] Links among observed CO_2 mole fraction, satellite-derived measures of plant growth, and agricultural inventory statistics corroborate the ability of the mole fraction to record crop management- and climate-induced changes in carbon flux. We are able to detect both regional-scale flooding effects and more subtle climate-induced changes in the timing of plant growth.

[34] From a monitoring perspective, it is the spatially and time-dependent regional flux determined from CO_2 mole fraction measurements and inversion models that is necessary to evaluate inventory methods. The uptake of CO_2 of corn and other crops compared to natural ecosystems during the growing season leads to a large-scale minimum of CO_2 mole fraction in the MCI region [*Corbin et al.*, 2010]. The NEE over the course of the year (on the larger, national scale) is almost zero, since crops are harvested, transported, and used for food and livestock feed, and the crop residues decompose during the dormant season [*West et al.*, 2011]. Assessing the ability of inversion models to determine the regional flux is the focus of current research [e.g., *Lauvaux et al.*, 2011].

[35] In summary, these results suggest that a limited number of samples across the corn belt of the U.S. upper Midwest captured the dominant spatial patterns in CO_2 mole fraction. In this region with extensively documented inventory data, spatial and temporal variability in CO_2 fluxes was concurrently recorded in tower, inventory, and satellite data. Similar regional networks, deployed in other parts of the globe, are therefore highly likely to capture strong regional signals characteristic of CO_2 fluxes. Relatively simple, moderate-cost, ground-based networks, combined with mesoscale inverse modeling systems, could be an effective means of providing atmospheric verification of regional CO_2 emissions inventories.

[36] **Acknowledgments.** The authors gratefully acknowledge the tower owners for allowing tower access and for on-site help; without their cooperation this work would not have been possible. We thank T. Griffis (University of Minnesota) for providing Rosemount CO_2 mole fraction and flux data. We recognize P. Tans (NOAA-ESRL) for providing globally

averaged data and C. Sweeney (NOAA-ESRL) for providing West Branch aircraft data. We thank A. Schuh (Colorado State University) for providing biome maps. For eddy-covariance flux data we acknowledge A. Suyker and S. Verma (University of Nebraska at Lincoln) for Mead, R. Matamala (Argonne National Laboratory) for Fermi and Brookings, and L. Gu (Oak Ridge National Laboratory) for Missouri Ozarks. This research was sponsored by the U.S. Department of Energy Office of Science TCP Program (DE-FG02-06ER64315) and by the U.S. Department of Commerce, NOAA Office of Global Programs (NA08OAR4310533). Processing of MODIS NDVI was sponsored by the NASA Earth Sciences Division. MCI tower data are available online at http://www.ring2.psu.edu.

References

Bakwin, P. S., P. P. Tans, C. Zhao, W. Ussler, and E. Quesnell (1995), Measurements of carbon dioxide on a very tall tower, *Tellus, Ser. B*, *47*, 535–549, doi:10.1034/j.1600-0889.47.issue5.2.x.

Bakwin, P. S., P. P. Tans, D. F. Hurst, and C. Zhao (1998), Measurements of carbon dioxide on very tall towers: Results of the NOAA/CMDL program, *Tellus, Ser. B*, *50*, 401–415, doi:10.1034/j.1600-0889.1998.t01-4-00001.x.

Butler, M. P., K. J. Davis, A. S. Denning, and S. R. Kawa (2010), Using continental observations in global atmospheric inversions of CO_2: North American carbon sources and sinks, *Tellus, Ser. B*, *62*, 550–572, doi:10.1111/j.1600-0889.2010.00501.x.

Chan, D., C. W. Yuen, K. Higuchi, A. Shashkov, J. Liu, J. Chen, and D. Worthy (2004), On the CO_2 exchange between the atmosphere and the biosphere: The role of synoptic and mesoscale processes, *Tellus, Ser. B*, *56*, 194–212, doi:10.1111/j.1600-0889.2004.00104.x.

Chen, H., et al. (2010), High-accuracy continuous airborne measurements of greenhouse gases (CO_2 and CH_4) using the cavity ring-down spectroscopy technique, *Atmos. Meas. Tech.*, *3*, 375–386, doi:10.5194/amt-3-375-2010.

Committee on Methods for Estimating Greenhouse Gas Emissions (2010), *Verifying Greenhouse Gas Emissions: Methods to Support International Climate Agreements*, Natl. Res. Counc., Natl. Acad. Press, Washington, D. C. [Available at http://www.nap.edu.]

Corbin, K. D., A. S. Denning, E. Y. Lokupitiya, A. E. Schuh, N. L. Miles, K. J. Davis, S. Richardson, and I. T. Baker (2010), Assessing the impact of crops on regional CO_2 fluxes and atmospheric concentrations, *Tellus, Ser. B*, *62*, 521–532, doi:10.1111/j.1600-0889.2010.00485.x.

Crevoisier, C., C. Sweeney, M. Gloor, J. L. Sarmiento, and P. P. Tans (2010), Regional U.S. carbon sinks from three-dimensional atmospheric CO_2 sampling, *Proc. Natl. Acad. Sci. U. S. A.*, *107*, 18,348–18,353, doi:10.1073/pnas.0900062107.

Crosson, E. R. (2008), A cavity ring-down analyzer for measuring atmospheric levels of methane, carbon dioxide, and water vapor, *Appl. Phys. B*, *92*, 403–408, doi:10.1007/s00340-008-3135-y.

Davis, K. J., P. S. Bakwin, C. Yi, B. W. Berger, C. Zhao, R. M. Teclaw, and J. G. Isebrands (2003), The annual cycles of CO_2 and H_2O exchange over a northern mixed forest as observed from a very tall tower, *Global Change Biol.*, *9*, 1278–1293, doi:10.1046/j.1365-2486.2003.00672.x.

Denning, A. S. (Ed.) (2005), Science implementation strategy for the North American carbon program: Report of the NACP Implementation Strategy Group of the U.S. Carbon Cycle Interagency, report, U.S. Carbon Cycle Sci. Program, Washington, D. C. [Available at http://www.carboncyclescience.gov/documents/nacp_sis_2005.pdf.]

Dolman, A. J., et al. (2006), The CarboEurope Regional Experiment Strategy, *Bull. Am. Meteorol. Soc.*, *87*, 1367–1379, doi:10.1175/BAMS-87-10-1367.

Dwyer, J., and G. Schmidt (2006), The MODIS reprojection tool, in *Earth Science Satellite Remote Sensing*, edited by J. J. Qu et al., pp. 162–177, Springer, Berlin.

Gerbig, C., J. C. Lin, S. C. Wofsy, B. C. Daube, A. E. Andrews, B. B. Stephens, P. S. Bakwin, and C. A. Grainger (2003), Toward constraining regional scale fluxes of CO_2 with atmospheric observations over a continent: 1. Observed spatial variability from airborne platforms, *J. Geophys. Res.*, *108*(D24), 4756, doi:10.1029/2002JD003018.

Gerbig, C., A. J. Dolman, and M. Heimann (2009), On observational and modeling strategies targeted at regional carbon exchange over continents, *Biogeosciences*, *6*, 1949–1959, doi:10.5194/bg-6-1949-2009.

GLOBALVIEW-CO_2 (2011), *Cooperative Atmospheric Data Integration Project–Carbon Dioxide* [CD-ROM], NOAA Earth Syst. Res. Lab., Boulder, Colo.

Griffis, T. J., J. M. Baker, S. D. Sargent, M. Erickson, J. Corocoan, M. Chen, and K. Billmark (2010), Influence of C_4 vegetation on $^{13}CO_2$ discrimination and isoforcing in the upper Midwest, United States, *Global Biogeochem. Cycles*, *24*, GB4006, doi:10.1029/2009GB003768.

Gu, L., P. J. Hanson, W. M. Post, D. P. Kaiser, B. Yang, R. Nemani, S. G. Pallardy, and T. Meyers (2008), The 2007 eastern U.S. spring freezes: Increased cold damage in a warming world?, *Biosciences*, *58*, 253–262, doi:10.1641/B580311.

Gurney, K. R., D. L. Mendoza, Y. Zhou, M. L. Fischer, C. C. Miller, S. Geethakumar, and S. De La Rue Du Can (2009), High resolution fossil fuel combustion CO_2 emissions fluxes for the United States, *Environ. Sci. Technol.*, *43*, 5535–5541, doi:10.1021/es900806c.

Haszpra, L., Z. Barcza, D. Hidy, I. Szilágyi, E. Dlugokencky, and P. Tans (2008), Trends and temporal variations of major greenhouse gases at a rural site in Central Europe, *Atmos. Environ.*, *42*, 8707–8716, doi:10.1016/j.atmosenv.2008.09.012.

Houweling, S., et al. (2010), The importance of transport model uncertainties for the estimation of CO_2 sources and sinks using satellite measurements, *Atmos. Chem. Phys.*, *10*, 9981–9992, doi:10.5194/acp-10-9981-2010.

Hurwitz, M. D., D. M. Ricciuto, P. S. Bakwin, K. J. Davis, W. Wang, C. Yi, and M. P. Butler (2004), Transport of carbon dioxide in the presence of storm systems over a northern Wisconsin forest, *J. Atmos. Sci.*, *61*, 607–618, doi:10.1175/1520-0469(2004)061<0607:TOCDIT>2.0.CO;2.

Johnson, D. M., and R. Mueller (2010), The 2009 cropland data layer, *Photogramm. Eng. Remote Sens.*, *76*, 1201–1205.

King, A. W., L. Dilling, G. P. Zimmerman, D. M. Fairman, R. A. Houghton, G. Marland, A. Z. Rose, and T. J. Wilbanks (Eds.) (2007), The first State of the Carbon Cycle Report (SOCCR): The North American carbon budget and implications for the global carbon cycle, report, 242 pp., NOAA Natl. Clim. Data Cent., Asheville, N. C. [Available at http://cdiac.ornl.gov/SOCCR/.]

Lauvaux, T., M. Uliasz, C. Sarrat, F. Chevallier, P. Bousquet, C. Lac, K. J. Davis, P. Ciais, A. S. Denning, and P. J. Rayner (2008), Mesoscale inversion: First results from the CERES campaign with synthetic data, *Atmos. Chem. Phys.*, *8*, 3459–3471, doi:10.5194/acp-8-3459-2008.

Lauvaux, T., et al. (2009), Bridging the gap between atmospheric concentrations and local ecosystem measurements, *Geophys. Res. Lett.*, *36*, L19809, doi:10.1029/2009GL039574.

Lauvaux, T., et al. (2011), Constraining the CO_2 budget of the corn belt: Exploring uncertainties from the assumptions in a mesoscale inverse system, *Atmos. Chem. Phys.*, *12*, 337–354, doi:10.5194/acp-12-337-2012.

Lin, J. C., C. Gerbig, B. C. Daube, S. C. Wofsy, A. E. Andrews, S. A. Vay, and B. E. Anderson (2004), An empirical analysis of the spatial variability of atmospheric CO_2: Implications for inverse analysis and space-borne sensors, *Geophys. Res. Lett.*, *31*, L23104, doi:10.1029/2004GL020957.

Lokupitiya, E., A. S. Denning, K. Paustian, I. Baker, K. Schaefer, S. Verma, T. Meyers, C. Bernacchi, A. Suyker, and M. Fischer (2009), Incorporation of crop phenology in Simple Biosphere Model (SiBcrop) to improve land-atmosphere carbon exchanges from croplands, *Biogeosciences*, *6*, 969–986, doi:10.5194/bg-6-969-2009.

Martins, D. K., C. Sweeney, B. H. Stirm, and P. B. Shepson (2009), Regional surface flux of CO_2 interred from changes in the advected CO_2 column density, *Agric. For. Meteorol.*, *149*, 1674–1685, doi:10.1016/j.agrformet.2009.05.005.

Matamala, R., D. J. Jastrow, R. M. Miller, and C. Garten (2008), Temporal changes in the distribution of C and N stocks in a restored tallgrass prairie in the U.S. Midwest, *Ecol. Appl.*, *18*, 1470–1488, doi:10.1890/07-1609.1.

Matross, D. M., et al. (2006), Estimating regional carbon exchange in New England and Quebec by combining atmospheric, ground-based and satellite data, *Tellus, Ser. B*, *58*, 344–358, doi:10.1111/j.1600-0889.2006.00206.x.

Nisbet, E., and R. Weiss (2010), Top-down versus bottom-up, *Science*, *328*, 1241–1243, doi:10.1126/science.1189936.

Ogle, S., K. Davis, A. Andrews, K. Gurney, T. West, R. Cook, R. Parkin, J. Morisette, S. Verma, and S. Wofsy (2006), Science Plan: Mid-Continent Intensive Campaign, report, U.S. Global Change Res. Program, North Am. Carbon Program, Greenbelt, Md. [Available at http://www.nacarbon.org/nacp/mci.html.]

Ogle, S., F. J. Breidt, M. Easter, S. Williams, K. Killian, and K. Paustian (2010), Scale and uncertainty in modeled soil organic carbon stock changes for U.S. croplands using a process-based model, *Global Change Biol.*, *16*, 810–822, doi:10.1111/j.1365-2486.2009.01951.x.

Peters, W., et al. (2007), An atmospheric perspective on North American carbon dioxide exchange: CarbonTracker, *Proc. Natl. Acad. Sci. U. S. A.*, *104*, 18,925–18,930, doi:10.1073/pnas.0708986104.

Peylin, P., P. J. Rayner, P. Bousquet, C. Carouge, F. Hourdin, P. Heinrich, P. Ciais, and AEROCARB contributors (2005), Daily CO_2 flux estimates over Europe from continuous atmospheric measurements: 1, Inverse methodology, *Atmos. Chem. Phys.*, *5*, 3173–3186, doi:10.5194/acp-5-3173-2005.

Richardson, S. J., N. L. Miles, K. J. Davis, E. R. Crosson, C. Rella, and A. E. Andrews (2012), Field testing of cavity ring-down spectroscopy

analyzers measuring carbon dioxide and water vapor, *J. Atmos. Oceanic Technol.*, doi:10.1175/jtech-d-11-00063.1, in press.

Schuh, A. E., A. S. Denning, K. D. Corbin, I. T. Baker, M. Uliasz, N. Parazoo, A. E. Andrews, and D. E. J. Worthy (2010), A regional high-resolution carbon flux inversion of North America for 2004, *Biogeosciences*, *7*, 1625–1644, doi:10.5194/bg-7-1625-2010.

Skamarock, W. C., J. B. Klemp, J. Dudhia, D. O. Gill, D. M. Barker, M. Duda, X.-Y. Huang, W. Wang, and J. G. Powers (2008), A description of the Advanced Research WRF version 3, *NCAR Tech. Note 475+STR*, Natl. Cent. for Atmos. Res., Boulder, Colo.

Stephens, B. B., N. L. Miles, S. J. Richardson, A. S. Watt, and K. J. Davis (2011), Atmospheric CO_2 monitoring with single-cell NDIR-based analyzers, *Atmos. Meas. Tech.*, *4*, 2737–2748, doi:10.5194/amt-4-2737-2011.

Tans, P. P., I. Y. Fung, and T. Takahashi (1990), Observational constraints on the global atmospheric CO_2 budget, *Science*, *247*, 1431–1438, doi:10.1126/science.247.4949.1431.

Tolk, L. F., W. Peters, A. G. C. A. Meesters, M. Groenendijk, A. T. Vermeulen, G. J. Steeneveld, and A. J. Dolman (2009), Modelling regional scale surface fluxes, meteorology and CO_2 mixing ratios for the Cabauw tower in the Netherlands, *Biogeosciences*, *6*, 2265–2280, doi:10.5194/bg-6-2265-2009.

Uliasz, M. (1994), *Lagrangian Particle Modeling in Mesoscale Applications, Environmental Modelling II*, edited by P. Zanetti, pp. 71–102, Comput. Mech. Publ., Southampton, U. K.

U.S. Department of Agriculture-National Agricultural Statistics Service (USDA-NASS) (2010), Quick Stats Database, http://www.nass.usda.gov/Data_and_Statistics/Quick_Stats/index.asp, Washington, D. C.

Verma, S. B., et al. (2005), Annual carbon dioxide exchange in irrigated and rainfed maize-based agroecosystems, *Agric. For. Meteorol.*, *131*, 77–96, doi:10.1016/j.agrformet.2005.05.003.

Vermote, E. F., N. Z. El Saluous, and C. O. Justice (2002), Atmospheric correction of MODIS data in the visible to near infrared: First results, *Remote Sens. Environ.*, *83*, 97–111, doi:10.1016/S0034-4257(02)00089-5.

Vermote, E. F., S. Y. Kotchenova, and J. P. Ray (2011), MODIS surface reflectance user's guide, v. 1.3, user's manual, MODIS Land Surface Reflectance Sci. Comput. Facil., NASA, Greenbelt, Md. [Available at http://modis-sr.ltdri.org/products/MOD09_UserGuide_v1_3.pdf.]

Wang, J.-W., A. S. Denning, L. Liu, I. T. Baker, K. D. Corbin, and K. J. Davis (2007), Observations and simulations of synoptic, regional and local variations in atmospheric CO_2, *J. Geophys. Res.*, *112*, D04108, doi:10.1029/2006JD007410.

West, T. O., C. C. Brandt, B. S. Wilson, C. M. Hellwinckel, D. D. Tyler, G. Marland, D. G. De La Torre Ugarte, J. A. Larson, and R. Nelson (2008), Estimating regional changes in soil carbon with high spatial resolution, *Soil Sci. Soc. Am. J.*, *72*, 285–294, doi:10.2136/sssaj2007.0113.

West, T. O., et al. (2010), Cropland carbon fluxes in the United States: Increasing resolution of inventory-based carbon accounting, *Ecol. Appl.*, *20*, 1074–1086, doi:10.1890/08-2352.1.

West, T. O., V. Bandaru, C. C. Brandt, A. E. Schuh, and S. M. Ogle (2011), Regional uptake and release of crop carbon in the United States, *Biogeosciences*, *8*, 2037–2046, doi:10.5194/bg-8-2037-2011.

Wofsy, S. C., and R. C. Harriss (2002), The North American Carbon Program (NACP), report, U.S. Global Change Res. Program, Washington, D. C.

Wolfe, R. E., M. Nishihama, A. J. Fleig, J. A. Kuyper, D. P. Roy, J. C. Storey, and F. S. Patt (2002), Achieving sub-pixel geolocation accuracy in support of MODIS land science, *Remote Sens. Environ.*, *83*, 31–49, doi:10.1016/S0034-4257(02)00085-8.

Xiao, J., et al. (2008), Estimation of net ecosystem carbon exchange for the conterminous United States by combining MODIS and AmeriFlux data, *Agric. For. Meteorol.*, *148*, 1827–1847, doi:10.1016/j.agrformet.2008.06.015.

Zhao, C., P. S. Bakwin, and P. P. Tans (1997), A design for unattended monitoring of trace gases on a tall tower, *J. Atmos. Oceanic Technol.*, *14*, 1139–1145, doi:10.1175/1520-0426(1997)014<1139:ADFUMO>2.0.CO;2.

A. E. Andrews, Earth System Research Laboratory, Global Monitoring Division, National Oceanic and Atmospheric Administration, 325 Broadway, R/GMD1, Boulder, CO 80305, USA.

V. Bandaru and T. O. West, Pacific Northwest National Laboratory, Joint Global Change Research Institute, University of Maryland, 5825 University Research Ct., Ste. 3500, College Park, MD 20740, USA.

E. R. Crosson, Picarro, Inc., 480 Oakmead Pkwy., Sunnyvale, CA 94085, USA.

K. J. Davis, T. Lauvaux, N. L. Miles, and S. J. Richardson, Department of Meteorology, Pennsylvania State University, 503 Walker Bldg., University Park, PA 16802, USA. (nmiles@met.psu.edu)